

Precoding for Joint Spectral Sidelobes Suppression and PAPR Reduction in OFDM System

Lei Wang, Lei Zhang*, Renhui Xu, Laixian Peng

College of Communication Engineering
PLA University of Science and Technology
Nanjing, China 210007

e-mail: raywangl@163.com, leizhang@163.com, xurenhui@aa.seu.edu.cn, penglaixian@sina.com

Abstract—In the scenario of multiple access communication, the spectral sidelobes and peak-to-average power ratio (PAPR) problems of orthogonal frequency division multiplexing (OFDM) must not be ignored. This paper proposes a novel precoding scheme that ahead of inverse discrete Fourier transformation (IDFT) is presented to jointly suppress the in-band-out-of-subband (IBOSB) radiation and high PAPR in orthogonal frequency division multiplexing access (OFDMA) systems. Its design is based on generalized eigenvalue problem. Finally, the results of simulations show that joint precoding scheme achieves the markedly performance of spectral sidelobes suppression and PAPR reduction.

Keywords—OFDM; precoding; OOB radiation; sidelobe suppression; PAPR; PAPR reduction; joint precoding

I. INTRODUCTION

OFDM is the most popular multicarrier transmission technique and it is widely used in most of the existing broadband communication standards, such as Digital audio broadcasting, standard (DAB), Digital video broadcasting standard (DVB), Wi-Fi, WiMAX, LTE, Digital subscriber line (DSL), IEEE802.22 WRAN and so on. For broadband communication application, OFDM is regarded as the promising candidates because of its numerous advantages such as high spectral efficiency, tolerance to multipath fading, waveform agility, and simple equalization. However, OFDM also suffers out-of-band (OOB) radiation and high PAPR problems. Both of these problems have a large impact on the performance of OFDM and greatly limit its practical applications. For instance, the IBOSB radiation, if not taken into account, can create interference to adjacent users. The OOB radiation is due to the block-wise IDFT operation [1], which is equivalent to multiplying the symbol block with a rectangular window in time domain, leads to a *sinc*-shaped spectrum of each subcarriers. As for high PAPR, if not reduced, the power amplifier (PA) operates in the nonlinear region of the radio-frequency (RF) components and creates both spectrum regrowth and self-distortion in the transmitted signal [2]. The PAPR is due to that OFDM signals are composed of multiple subcarriers with independent amplitudes and phase, that when add together are more likely to generate a signal with high peak power [3]. Thereby, the spectral sidelobes and high PAPR problems attracts much attention.

Both of OOB spectral sidelobes and high PAPR problems are often treated separately in literatures [4]-[7],

when one problem is solved, the other remains, or becomes worse. For example, spectral sidelobes can regrowth after the high peak power transmitted signal passes through the PA [8], [9]. So the best way is to jointly suppress spectral sidelobes and reduce PAPR as done in [10]-[13] and the references therein. Among the joint reduction techniques, the selected mapping (SLM) scheme is employed to generate several alternative signals and selected the signal with low PAPR and sidelobes as the transmitted signal [14], [15]. While signal cancelation (SC) method's key idea is to dynamically expand part of the constellation points on the secondary user (SU) subcarriers and add several SC symbols on the primary user (PU) subcarriers to generate the appropriate cancelation signal for joint PAPR reduction and sidelobes suppression [16], and reserved tones (RTs) technique uses a signal set of carriers, which do not carry data, but are modulated with complex weighting factors such that both spectral sidelobes and PAPR of data carriers are reduced [17]. Besides, partial transmit sequence (PTs) is to generate some phase factors that meet to constraints of the joint optimization problem to minimize PAPR with a constraint on the maximum tolerable sidelobes power [18], [19]. Almost all of the aforementioned joint reduction techniques suffer from either a spectral efficiency loss or bit error rate (BER) degradation, and are more complexity compared with pure OFDM systems.

In the past years, a novel precoding scheme is proposed to produce significant either individual suppression in the spectral sidelobes [20] or reduction in the high PAPR [6], or joint reduction [21]. In this paper, a joint precoding scheme is proposed to jointly suppress the IBOSB radiation and high PAPR in an unlinked communication network of OFDMA scenario with K transmit nodes (users) and 1 receiving node (base station), OFDM modulation is chosen for its physical layer transport protocol. In the OFDM systems, frequency spectrum B is equally divided into N subcarriers with indices $n \in B (B = [0, \dots, N-1])$ and K subsets of subcarriers, so the size of subsets is $P = N/K$. Every user is assigned a subset and the users' indices $k = 1, 2, \dots, K$. For the k th user, the subcarriers' indices $B_k = [(k-1)P, kP-1]$. The sidelobe power of the k th user in B_k spills to $B_u (u \neq k)$ is denoted as the IBOSB (in-band-out-of-subband) radiation (or IBOSB interference).

The rest of the paper is organized as follows. In section II, the joint precoding scheme is overviewed in brief. The concept of PAPR reduction algorithm and IBOSB suppression as well as joint suppression is presented in section III. The numerical simulation results on signal spectrum and PAPR on multipath fading channel is provided in section IV. Finally, the conclusion is given in Section V.

Notations: I_P is the $P \times P$ identity matrix; $0_{P \times P}$ is an all zeroes $P \times P$ matrix. The transpose and conjugate transpose are denoted by $(\cdot)^T$ and $(\cdot)^H$. Respectively, $\|\cdot\|_2$ denotes the 2-norm and $\|\cdot\|_\infty$ denotes the uniform norm. Besides, $\text{tr}(\cdot)$ denotes trace and $E[\cdot]$ denotes the expectation operator.

II. SYSTEM MODEL WITH PRECODING

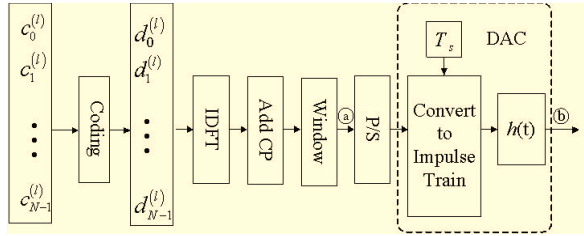


Figure 1. DFT-based OFDM system block diagram

A typical OFDM transmitter with precoding [20] based on DFT-based implementation is shown in Figure 1. The period of OFDM symbol is defined T , so the frequency interval between subcarrier is $\Delta f = 1/T$. The symbol block index is l , and $\mathbf{c}^{(k,l)} = [c_0^{(k,l)}, c_1^{(k,l)}, \dots, c_{P-1}^{(k,l)}]^T$ is the l th length- M modulated data column vector of k th user. The original modulated data of each OFDM block is preprocessed by a precoding matrix before IDFT into $\mathbf{d}^{(l)} = [d_0^{(k,l)}, d_1^{(k,l)}, \dots, d_{P-1}^{(k,l)}]^T$ via the precoding

$$\mathbf{d}^{(l)} = \mathbf{G}^{(k)} \mathbf{c}^{(l)} \quad (1)$$

where $\mathbf{G}^{(k)} = \{\mathbf{g}_{n,m}^k\}$ is precoding matrix of k th user with size of $P \times P$, $d^{(k,l)}$ is the l th modulated data with precoding of k th user, and it is column vector with size of $P \times 1$. Then map precoding data of k th user into addressed subcarriers via the matrix $\mathbf{M} = (0_{P \times P}^{(1)}, 0_{P \times P}^{(2)}, \dots, I_P^{(k)}, \dots, 0_{P \times P}^{(K)})^T$.

After through IDFT (with DFT-size N) and cyclic prefix (CP) insertion (with CP length ν), the resultant discrete sampled values of serial data streams with length $L = N + \nu$,

$$x[s] = \frac{1}{\sqrt{N}} \sum_{l=-\infty}^{\infty} \sum_{n=(k-1)P}^{kP-1} d_n^{(k,l)} e^{j2\pi(s-\nu-ll)N/N} w_L[s-ll] \quad (2)$$

where indices $s=0,1,\dots,S-1$, w_L denotes discrete time domain window functions. After parallel-to-serial (P/S) conversion, the discrete time Fourier transform (DTFT) of the window function can be expressed as $w_L(e^{j\omega T_s})$ with sampling period is $T_s = 1/(N\Delta f)$. Then the digital analog converter (DAC) outputs the complex envelope of the DFT-based baseband OFDM signal

$$b(t) = \sum_{l=-\infty}^{+\infty} \sum_{s=-\infty}^{+\infty} x[s] h(t - sT_s) \quad (3)$$

where $h(t)$ is reconstruction filter and $H(j\omega)$ denotes the continuous-time Fourier transform of $h(t)$. Then the spectrum of baseband OFDM signal is calculated as

$$B^{(k)}(j\Omega) = \frac{1}{\sqrt{N}} H(j\Omega) \sum_{n=(k-1)P}^{kP-1} d_n^{(k)} e^{-j2\pi\Omega n/N} \bullet \sum_{s=0}^{L-1} w_L[s] e^{j2\pi\Omega s/N} e^{-j\Omega s T_s} \quad (4)$$

which can be described as the sum of the spectrum of individual N subcarriers, which are *sinc*-like-shaped functions.

Assuming the modulated data $\mathbf{c}^{(l)}$ contains the complex variables from a given MPSK (Multiple Phase-Shift-Keying) constellation, and has the mean $E(\mathbf{c}) = \mathbf{0}$ and covariance $\text{Var}(\mathbf{c}) = \sigma^2 \mathbf{I}_M$ with \mathbf{I}_M being $M \times M$ identity matrix. Consequently, the power spectrum of $b(t)$ is given by

$$S^{(k)}(j\Omega) = \frac{\sigma^2}{N} |H(j\Omega)|^2 \bullet \left| \sum_{n=(k-1)P}^{kP-1} g_{n,m}^{(k)} e^{-j2\pi\Omega n/N} \right| \quad (5)$$

$$\sum_{s=0}^{L-1} w_L[s] e^{j2\pi\Omega s/N} e^{-j\Omega s T_s} \right|^2$$

Alternatively, (4) can be written in vector-matrix form as

$$B^{(k)}(j\Omega) = \frac{1}{\sqrt{N}} H(j\Omega) \mathbf{e}^H \mathbf{W} \mathbf{D}^{(k)} \mathbf{c}^{(k)} \quad (6)$$

where \mathbf{e} is a $L \times 1$ vector with the k th entry $e^{j\Omega T_s}$, $\mathbf{W} = \mathbf{w} \mathbf{F}^H$ with $\mathbf{w} = \text{diag}(w_L[0], w_L[1], \dots, w_L[L-1])$ and \mathbf{F} is a Fourier

matrix with the (n,k) th entry $[\mathbf{F}]_{n,k} = \frac{1}{\sqrt{N}} e^{j2\pi\Omega n/N}$. Besides,

$\mathbf{D} = \text{diag}(1, e^{-j2\pi\Omega \nu/N}, \dots, e^{-j2\pi\Omega \nu/N}, \dots, e^{-j2\pi\Omega \nu(N-1)/N})$ and $\mathbf{D}^{(k)} = \mathbf{D} \mathbf{M} \mathbf{G}^{(k)}$. So (5) can be written in vector-matrix form as

$$S^{(k)}(j\Omega) = \frac{\sigma^2}{N} |H(j\Omega)|^2 \|\mathbf{e}^H \mathbf{W} \mathbf{D}^{(k)}\|_2^2 \quad (7)$$

or

$$S^{(k)}(j\Omega) = \frac{\sigma^2}{N} |H(j\Omega)|^2 \text{tr}(\mathbf{D}^{(k)H} \mathbf{W}^H \mathbf{e} \mathbf{e}^H \mathbf{W} \mathbf{D}^{(k)}) \quad (8)$$

III. JOINT PRECODING SUPPRESSION

A. IBOSB Suppression

Considering the interference of k th user to multiple users in the networks, the power spectrum of $b(t)$ needs to be controlled to suppress spectral sidelobes of in-band-out-of-subband (IBOSB) radiation. Under the condition of certain signal power, in order to minimize the power of the out of band radiation, it is equivalent to maximum power in the user data subband. A maximum problem is constructed as

$$\arg \max_G \text{tr}(\mathbf{G}^{(k)H} \mathbf{A} \mathbf{G}^{(k)}) \quad (9)$$

where $\mathbf{A} = \mathbf{M}^H \mathbf{D}^H \mathbf{W}^H \mathbf{P} \mathbf{W} \mathbf{D} \mathbf{M}$ are Hermitian matrices with $\mathbf{P} = \int_{\Xi} \mathbf{e} \mathbf{e}^H d\Omega / 2\pi$ and $\Xi \in [(k-1)P, kP-1]_{\Delta f}$.

It is treated as a generalized Hermitian eigenvalue problem. The precoding \mathbf{G} satisfies the orthogonality constraint, which guarantees that the power is invariant during the precoding [20].

B. PAPR Reduction

The other important characteristics of the OFDM transmitted signals is PAPR, which can be defined as

$$\text{PAPR} = \frac{\max |b(t)|^2}{E[|b(t)|^2]} \quad (10)$$

where $\max |b(t)|^2$ is the maximum instantaneous power of the OFDM signal. The continuous-time PAPR can be approximated by the discrete PAPR with oversampling on $b(t)$. The discrete-time OFDM signal with oversampling factor a is given by

$$x[s] = \frac{1}{\sqrt{N}} \sum_{l=-\infty}^{\infty} \sum_{n=(k-1)P}^{kP-1} \left(d_n^{(k,l)} e^{j2\pi(s-v-LL)n/aN} \cdot w_L[s-lL] \right) \quad (11)$$

where the discrete time-domain signal $x[s]$ has an indices of $[0, \dots, aL-1]$. Usually, the oversampling factor can take an integer such that $a \geq 4$ for $\text{PAPR}(x[s])$ to approach the actual PAPR of the continuous-time signal. Consequently, the PAPR can also be approximate defined as

$$\text{PAPR} = \frac{\max |x[s]|^2}{E[|x[s]|^2]} \quad (12)$$

The performance evaluation index of PAPR is the complementary cumulative distribution function (CCDF), which is defined as

$$\text{CCDF} = \text{Pr}(\text{PAPR} > \lambda) \quad (13)$$

where λ is to measure the threshold of PAPR. In order to reduce PAPR, the precoding matrix \mathbf{G} is defined to optimize the following functions:

$$\arg \min_G \frac{\|\mathbf{W} \mathbf{D} \mathbf{c}^{(k)}\|_{\infty}^2}{\frac{1}{L} \|\mathbf{W} \mathbf{D} \mathbf{c}^{(k)}\|_2^2} \quad (14)$$

It is treated as a mathematical autocorrelation function problem. The magnitude of the PAPR value is related to the mathematical autocorrelation matrix of the input signal, and the precoding is designed to adjust the mathematical autocorrelation of the input data of the IFFT modulation to achieve the purpose of PAPR reduction.

C. Joint Suppression

Combined with (9) and (14), the optimal objective function of joint OOB and PAPR suppression is obtained as

$$\begin{cases} \arg \max_G \text{tr}(\mathbf{G}^{(k)H} \mathbf{A} \mathbf{G}^{(k)}) \\ \arg \min_G \frac{\|\mathbf{W} \mathbf{D} \mathbf{c}^{(k)}\|_{\infty}^2}{\frac{1}{L} \|\mathbf{W} \mathbf{D} \mathbf{c}^{(k)}\|_2^2} \end{cases} \quad (15)$$

To avoid the BER performance degradation because of noise amplification by the decoder \mathbf{G} , we prefer to use a precoder \mathbf{G} of which all singular values are one. This condition will be referred as 'the constant singular value condition' and is imposed on the precoder design in our approaches. It is known that a semi-unitary matrix \mathbf{G} (i.e. $\mathbf{G}^H \mathbf{G} = \mathbf{I}$) satisfies the 'constant singular value condition' (the non-zero singular values of a semi-unitary matrix are one) [21].

To simplify the analysis and calculation, first separately considering the OOB suppression and PAPR suppression by sub-precoding matrix \mathbf{G}^* and \mathbf{S}^* , so precoding matrix \mathbf{G} can be defined as

$$\mathbf{G} = \mathbf{G}^* \mathbf{S}^* \quad (16)$$

For sub-precoding matrix \mathbf{S}^* , there are two conditions should be satisfied as follows.

- 1) Sub-precoding matrix \mathbf{S}^* had no effect on the performance of sub-precoding matrix \mathbf{G}^* for OOB suppression;
- 2) Sub-precoding matrix \mathbf{S}^* is a semi-unitary matrix.

A special sub-precoding matrix \mathbf{S}^* is each column vector with only a nonzero element whose value is 1, then the sub-precoding matrix \mathbf{S}^* right multiply sub-precoding matrix \mathbf{G}^* is equivalent to adjust precoding matrix \mathbf{G}^* 's columns to achieve optimal PAPR. A search optimal algorithm of sub-precoding (SOSP) matrix \mathbf{S}^* is described as follows.

- 1) Initialize the iterative number with $k=0$. Original sub-precoding matrix $\mathbf{S}^* = \mathbf{I} = [\mathbf{g}_0 \ \mathbf{g}_1 \ \dots \ \mathbf{g}_{P-1}]$, where $\mathbf{g}_i = (\mathbf{0} \ \mathbf{0} \ \dots \ \mathbf{1} \ \dots \ \mathbf{0})^T$, the value of $(i+1)$ th element is 1 and the other element is 0, and $i = 0, 1, \dots, P-1$.
- 2)
 - a) Initialize the iterative number with $m=k$, substitute \mathbf{G} into (1) and compute the PAPR through (12) equal to PAPR_{\min} , record $\mathbf{m}_{\min} = m$;
 - b) Exchange \mathbf{g}_k and \mathbf{g}_m and obtain new sub-precoding matrix \mathbf{S}^* , then substitute new \mathbf{S}^* into (16) obtain new precoding matrix \mathbf{G} .
 - c) Substitute \mathbf{G} into (1) and recompute the PAPR Through (12), exchange \mathbf{g}_k and \mathbf{g}_m to recover initial sub-precoding \mathbf{S}^* ,
If $\text{PAPR} < \text{PAPR}_{\min}$, then

Update $\text{PAPR}_{\min} = \text{PAPR}$, record $\mathbf{m}_{\min} = m$;

```

        goto d);
    else
        goto d);
    end if
d) if  $m$  arrive at the maximum iteration number,
    then
        goto e);
    else
         $m := m + 1$ ;
        goto b);
    end if
e) Exchange  $\mathbf{g}_k$  and  $\mathbf{g}_m$  and obtain new sub-
    precoding matrix  $\mathbf{S}^*$ .
3) if  $k$  arrive at the maximum iteration number, then
    Obtain new precoding matrix  $\mathbf{G}$  through (16);
    goto 4);
else
     $k := k + 1$ ;
    goto 2);
end if
4) End Put  $\mathbf{d}^{(k)} = \mathbf{G}^{(k)} \mathbf{c}^{(k)}$  into IDFT.

```

IV. SYSTEM PERFORMANCE

To illustrate the performance improvement of the proposed scheme, some simulation results are presented in this section. A simple spectrum pooling scenario identical to [20] holds a frequency band with 2.5MHz , which is divided into four equal-wide subbands. All 4 subbands with $N = 128$ OFDM subcarriers, *i.e.*, 32 subcarriers each subband. The 2nd user is observed and using the 2nd subband. Assume the CP length to be $N/4$, and set the precoding efficiency as $\rho = 28/32$.

To evaluate the property of the transmitted analog OFDM signal, the discrete symbols pass through 4-times oversampling, rectangularly pulse shaping, ideal low pass filter (LPF) and HPA. To simulate the HPA, the following model is used for the AM/PM conversion [22]:

$$g[b(t)] = \frac{b(t)}{[1 + b(t)^{2p}]^{1/2p}} \quad (17)$$

where the index p is chosen as 3. The AM/PM conversion of HPA is neglected. In simulation, the HPA operates in low IBO (input back-off) of 4.5dB to observe the phenomenon of distorted signal leading to spectrum regrowth.

Four schemes are compared here. The first is conventional OFDM, the second is pure precoding and the third is precoding with selected column inverted (PSCI) in [20], and the fourth is precoding with search optimal algorithm of sub-precoding (SOSP). For the first scheme, additional two subcarriers on each end of subbands are deactivated in order to ensure the spectrum efficiency same as ρ of the precoding. For the second scheme, it is a pure precoding scheme without PAPR reduction algorithm. For the third scheme, the threshold PAPR in PSCI algorithm is set as 3dB. For the fourth scheme, it is a precoding with

PAPR reduction algorithm which is proposed in this paper. All results shown are averaged over 10^5 OFDM blocks and the block energy of various scheme is normalized to be identical for fair comparison.

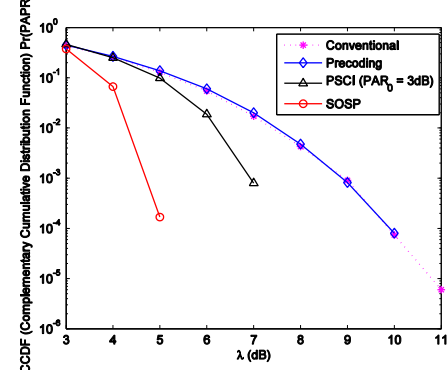


Figure 2. Complementary cumulative distribution function of the PAPR

Figure 2 shows the PAPR measurement of the four schemes in terms of CCDF (complementary cumulative distribution function), which is defined as $Pr(PAPR > \lambda)$. It is observed that PSCI with threshold $PAPR = 3\text{dB}$ provides 2dB gain at CCDF value of 10^{-4} compared to the first conventional and the second pure precoding schemes, while SOSP scheme provides 3dB gain at CCDF value of 10^{-4} compared to the third PSCI scheme. Compared to the first conventional and the second pure precoding schemes, SOSP scheme provides 5dB gain at CCDF value of 10^{-4} . The numerical results prove that the SOSP scheme indeed can achieve a greater improvement in PAPR reduction performance.

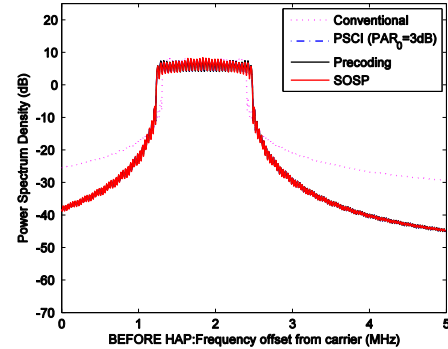


Figure 3. Power spectrum density comparison of signal before HPA

Figure 3 and Figure 4 presents the comparison on the power spectrum of the signal before and after HPA respectively. Comparing Figure 3 with Figure 4, we can observe that nonlinearity of the amplifier takes effect on the spectrum of the conventional OFDM and the pure precoding, for the spectral leakage of both schemes in the 2nd subband is increased a little. The spectral leakage regrowth is due to the high peak power amplified in non-linear region of HPA. And the pure precoding seems to be more vulnerable to the peak distortion than the other three methods, although it suppresses more IBOSB radiation than the conventional

OFDM. Before HPA, compared with the conventional OFDM, the precoding method can achieve a greater IBOSB suppression. For pure precoding, precoding combined with PAPR reduction of PSCI and SOSP, these three schemes have a similar IBOSB suppression performance. These three schemes of simulation results are mutually overlapping which can be seen from Figure 3. But after HPA, for four schemes, the better performance of PAPR reduction, the better performance of IBOSB suppression. For SOSP scheme, it provides the best PAPR reduction compared to the other three schemes, so it have the best IBOSB suppression in four schemes. The advantage of SOSP lies in that the spectrum ripples have been smoothed compared with the other schemes.

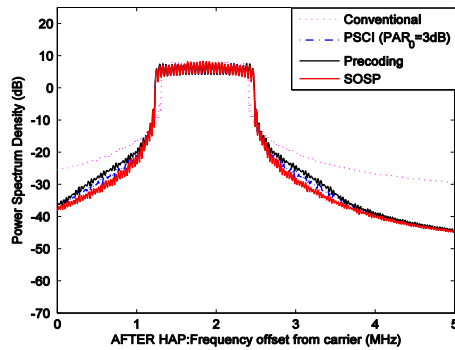


Figure 4. Power spectrum density comparison of signal after HPA

V. CONCLUSION

In this paper, we proposed a precoding approach for joint spectral sidelobes suppression and PAPR reduction in OFDM systems. Simulations confirm the effectiveness of joint design. The SOSP method for PAPR reduction provides a greatly performance improvement, while also has beneficial effect on precoding for IBOSB suppression. But the precoding schemes if have impact on BER performance of OFDM system without consideration. In the next work, the joint precoding schemes if have impact on BER performance of OFDM system will be analyzed, and the BER simulation of the joint precoding will be gave.

ACKNOWLEDGMENT

This work is supported by National Nature Science Foundation of China (No. 61671471).

REFERENCES

- [1] Y.-P. Lin and S.-M. Phoong, "Ofdm transmitters: analog representation and dft-based implementation," *IEEE Transactions on Signal Processing*, vol. 51, no. 9, pp. 2450–2453, Sept 2003.
- [2] A. Rady, M. El-Sayed, El-Rabaie, M. Shokair, and A. Elkorany, "Joint sidelobe suppression and papr reduction techniques in ofdm-based cognitive radios, a literature review," 2016.
- [3] A. Tom and A. Sahin, "Suppressing alignment: Joint papr and out-of-band power leakage reduction for ofdm-based systems," *IEEE Transactions on Communications*, vol. 64, no. 3, pp. 1100–1109, March 2016.
- [4] A. Tom, A. Sahin, and H. Arslan, "Suppressing alignment: An approach for out-of-band interference reduction in ofdm systems," in 2015 IEEE International Conference on Communications (ICC), June 2015, pp.4630–4634.
- [5] J. Song and H. Ochiai, "Performance analysis for ofdm signals with peak cancellation," *IEEE Transactions on Communications*, vol. 64, no. 1, pp.261–270, Jan 2016.
- [6] S. B. Slimane, "Reducing the peak-to-average power ratio of ofdm signals through precoding," *IEEE Transactions on Vehicular Technology*, vol. 56, no. 2, pp. 686–695, March 2007.
- [7] C. D. Chung and K. Chen, "Spectrally precoded ofdm without guard insertion," *IEEE Transactions on Vehicular Technology*, vol. PP, no. 99, pp. 1–1, 2016.
- [8] M. W. Chia, Y. Zeng, and Y.-C. Liang, "Closed-form approximations to the out-of-band emission due to nonlinear power amplifier," in 2013 IEEE Wireless Communications and Networking Conference (WCNC), April 2013, pp. 4032–4036.
- [9] T. Jiang, C. Li, and C. Ni, "Effect of papr reduction on spectrum and energy efficiencies in ofdm systems with class-a hpa over awgn channel," *IEEE Transactions on Broadcasting*, vol. 59, no. 3, pp. 513–519, Sept 2013.
- [10] Y. Liu, L. Dong, and R. J. Marks, "Joint reduction of out-of-band power and peak-to-average power ratio for non-contiguous ofdm systems," in 2013 IEEE Global Communications Conference (GLOBECOM), Dec 2013, pp. 3493–3498.
- [11] L. Dong, Y. Liu, and R. J. Marks, "Reduction of out-of-band power and peak-to-average power ratio in ofdm-based cognitive radio using alternating projections," in 2013 Texas Symposium on Wireless and Microwave Circuits and Systems (WMCS), April 2013, pp. 1–4.
- [12] A. Rady, M. Shokair, and E. S. M. El-Rabaie, "Efficient technique for sidelobe suppression and papr reduction in ofdm-based cognitive radios," *Wireless Personal Communications*, vol. 83, no. 1, pp. 1–16, 2015.
- [13] P. Wei, L. Dan, C. Zhou, Y. Xiao, G. Wu, and S. Li, "Joint optimization of peak-to-average power ratio and spectral leakage in 5g multicarrier waveforms," *China Communications*, vol. 12, no. Supplement, pp. 83–92, December 2015.
- [14] Y. Wu, K. L. Man, and L. Sun, "Joint papr and sidelobe power reduction using optimum slm," in *Wireless Telecommunications Symposium 2012*, April 2012, pp. 1–6.
- [15] A. Ghassemi, L. Lampe, A. Attar, and T. A. Gulliver, "Joint sidelobe and peak power reduction in ofdm-based cognitive radio," in 2010 IEEE 72nd Vehicular Technology Conference - Fall, Sept 2010, pp. 1–5.
- [16] C. Ni, T. Jiang, and W. Peng, "Joint papr reduction and sidelobe suppression using signal cancellation in nc-ofdm-based cognitive radio systems," *IEEE Transactions on Vehicular Technology*, vol. 64, no. 3, pp. 964–972, March 2015.
- [17] M. Senst, M. Jordan, M. Dorpinghaus, M. Farber, G. Ascheid, and H. Meyr, "Joint reduction of peak-to-average power ratio and out-of-band power in ofdm systems," in *IEEE GLOBECOM 2007 – IEEE Global Telecommunications Conference*, Nov 2007, pp. 3812–3816.
- [18] E. Gvenkaya, A. Tom, and H. Arslan, "Joint sidelobe suppression and papr reduction in ofdm using partial transmit sequences," in *MILCOM 2013 - 2013 IEEE Military Communications Conference*, Nov 2013, pp.95–100.
- [19] A. S. Namitha and S. M. Sameer, "Joint papr and sidelobe reduction in non-contiguous ofdm based cognitive radio systems," in 2015 IEEE International Conference on Signal Processing, Informatics, Communication and Energy Systems (SPICES), Feb 2015, pp. 1–5.
- [20] R. Xu, M. Chen, H. Wang, and W. Yu, "Performance improvement of ofdm system with the spectrum-sidelobe-suppressed precoding," in 2010 IEEE 72nd Vehicular Technology Conference - Fall, Sept 2010, pp. 1–5.
- [21] J. Fang and I. T. Lu, "Precoder designs for jointly suppressing out-of-band emission and peak-to-average power ratio in an orthogonal frequency division multiplexing system," *IET Communications*, vol. 8, no. 10, pp. 1705–1713, July 2014.
- [22] R. Van Nee and R. Prasad, *OFDM for wireless multimedia communications*. Artech House, Inc. Norwood, MA, USA, 2000.